Acta Crystallographica Section C
Crystal Structure Communications
ISSN 0108-2701

Poly[diaquadi-μ_6-oxalato-μ_5-oxalato-chromium(III)rubidium(I)]: a new supramolecular isomer

Hamza Kherfi,[a] Malika Hamadène,[a] Achoura Guehria-Laïdoudi,[a]* Slimane Dahaoui[b] and Claude Lecomte[b]

[a]Laboratoire de Cristallographie-Thermodynamique, Faculté de Chimie, USTHB, BP 32 El-Alia Bab Ezzouar, 16111 Algiers, Algeria, and [b]CRM2 UMR-CNRS 7036, Institut Jean Barriol, Nancy-Université BP 239, 54506 Vandoeuvre-lés-Nancy Cedex, France
Correspondence e-mail: guehria_laidoudi@yahoo.fr

Received 18 January 2011
Accepted 15 February 2011
Online 4 March 2011

The title compound, $[CrRb(C_2O_4)_2(H_2O)_2]_n$, obtained under hydrothermal conditions and investigated structurally at 100 K, is a three-dimensional supramolecular isomer of the layered structure compound studied at room temperature. This novel polymer is built up from crosslinked hetero-bimetallic units. The linkage of alternating edge- and vertex-shared $RbO_7(H_2O)_2$ and $CrO_4(H_2O)_2$ polyhedra running along three different directions gives a dense packing. The two independent ligands display two η^4-chelation modes and two conventional carboxylate bridges. However, the pentadentate ligand connects the Cr^{III} and Rb^{I} ions through one O-atom bridge, while the hexadentate ligand exhibits an additional η^3-chelation and two O-atom bridges. Each coordinated water molecule forms an O-atom bridge between the two metals. Moreover, in the absence of protonated ligands, these water molecules act as donors through their four H atoms in strong-to-weak hydrogen bonds. This results in zigzag chains of alternating oxalate and aqua ligands parallel to the twofold screw axis. The six double oxalates known to date containing an alkali and Cr^{III} all present layered two-dimensional structures. In the series, this supramolecular isomer is the first three-dimensional framework.

Comment

In recent years, the design of new supramolecular architectures using dicarboxylic acids as linkers has received great attention (Rao *et al.*, 2004), opening a wide research field for the generation of coordination polymers with various dimensionalities (Janiak, 2003; Cheetham *et al.*, 2006). Built up from discrete binuclear entities, chains, layers or three-dimensional crosslinked polynuclear units, these polymers create various kind of voids, leading to solids also called metal–organic frameworks (MOFs; Tranchemontagne *et al.*, 2009). Their open structures exhibit porosity which can be successfully used in ion exchange and gas storage (Czaja *et al.*, 2009; Uemura *et al.*, 2009; Yaghi & Li, 1996; Robinson & Zaworotko, 1995; Hoskins & Robson, 1990; Murray *et al.*, 2009). In the resulting extended network, some intrinsic structural features govern the tuneability and functionality of these materials. Among them, metal–oxalate-based compounds occupy a particular place due to the variety of behaviours introduced by this simplest dicarboxylic acid. Therefore, the properties they can display range from controlled complex thermal decomposition for the development of metal oxide nanoparticles (Audebrand *et al.*, 2003) to induced electronic interactions, *via* their rich bridging coordination modes for the formation of magnetic and multiferroic crystals (Coronado *et al.*, 1996; Mosaad *et al.*, 1995; Price *et al.*, 2003; Zhang *et al.*, 2008; Schaack, 1990). Concerning the connectors, in reticular chemistry the use of two metals to obtain a specific hetero-metallic framework from individual components in solution remains a challenge in the areas of both crystal engineering and crystal structure (Wang & Cohen, 2009). In this context, and as part of our research concerning polymeric dicarboxylates (Aliouane *et al.*, 2007; Djehni *et al.*, 2007; Rahahlia *et al.*, 2007), we have selected alkali and transition metals. By providing several kinds of noncovalent interactions, including metal coordination, hydrogen bonding and ionic characteristics, they may extend the scope of potential applications. We report in this paper the structure of poly-[diaquadi-μ_6-oxalato-μ_5-oxalato-chromium(III)rubidium(I)], which is a supramolecular isomer of the rubidium chromium dioxalate dihydrate previously studied at room temperature (Kolitsch, 2004).

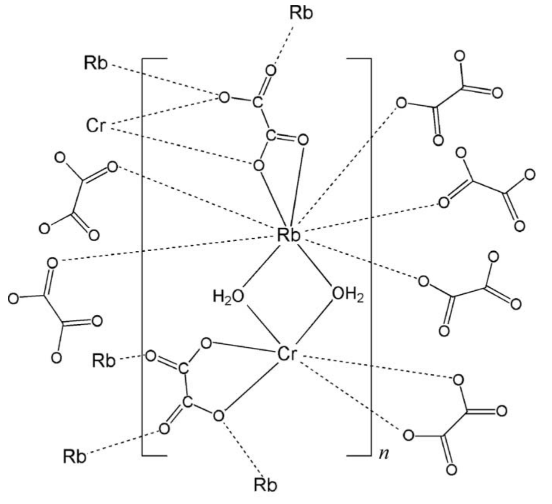

(I)

The structure of $[CrRb(C_2O_4)_2(H_2O)_2]_n$ is a three-dimensional MOF. The asymmetric unit corresponds to the chemical formula (see *Crystal data*). The structure is made up of RbO_7-$(H_2O)_2$ and $CrO_4(H_2O)_2$ polyhedra sharing edges through the two aqua ligands, without any solvent water. Although they are crystallographically independent, the two oxalate ligands are surrounded by the same number of metal ions (three different Rb^{I} atoms and one Cr^{III} atom) and present a rather

doi:10.1107/S0108270111005646

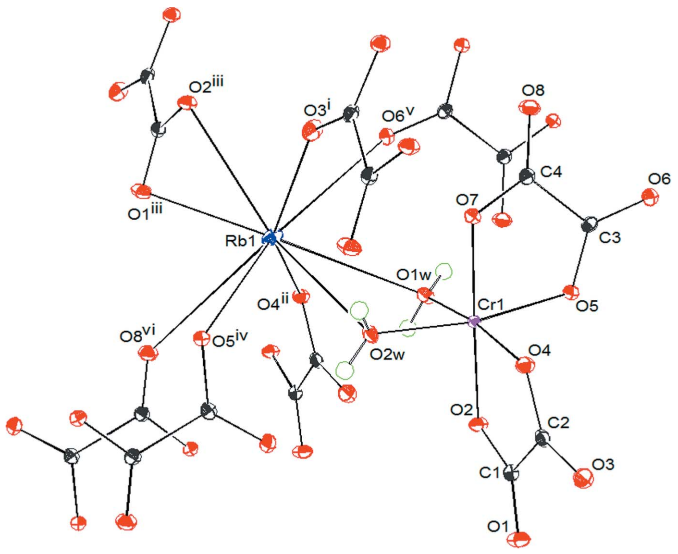

Figure 1
A segment of the polymeric structure, showing the environment around the metal atoms and the bridging positions of the water molecules. Displacement ellipsoids are drawn at the 50% probability level. (The symmetry codes are as in Table 1.)

usual *anti–anti* conformation (Table 1). They are approximately planar within experimental error; the largest deviations from the mean planes formed by the ligands *L*1 (atoms O1/O2/C1/C2/O3/O4) and *L*2 (O5/O6/C3/C4/O7/O8) are 0.0348 (11) and 0.1183 (11) Å, respectively, for atoms O2 and O5. They are nearly perpendicular to each other, the dihedral angle being 88.02 (5)°. However, ligand *L*2 is pentadentate, displaying two conventional μ-1,3 carboxylate bridges and an η^4-chelate so-called malonate mode, forming a five-membered ring (Cr1/O5/O3/C4/O7). Moreover, one end functional group is involved in a bridge through atom O5 and links together one Rb^{I} ion and one Cr^{III} ion. Like *L*2, *L*1 exhibits two conventional carboxylate bridges and one η^4-malonate mode formed by atoms Cr1/O4/C2/C1/O2. However, it is hexadentate, due to the two triply ligating atoms O4 and O2, which are involved in one O-atom bridge. Thus, this ligand is simultaneously η^4-chelating through its carbon backbone and η^3-chelating, with the alkali Rb^{I} ion, through one functional group (O1/C1/O2). To the best of our knowledge, this latter kind of chelate is very rare for alkali metals. Therefore, it can be reasonably assumed that the mainly electrostatic bonding commonly encountered with alkali cations is, in this case, behind the coordination character of the Rb—O linkage.

As seen in Fig. 1 and Table 1, the first coordination sphere of the Rb^{I} ion consists of seven O atoms from three *L*1, one *L*2 and two aqua ligands. In the second coordination sphere, two contacts greater than 3.11 Å are provided by two atoms [O6^{v} and O8^{vi}; symmetry codes: (v) $-x + 1, -y, -z + 1$; (vi) $-x + \frac{3}{2}, y + \frac{1}{2}, -z + \frac{3}{2}$] belonging to two different *L*2 ligands. The next longest Rb—O contact is 3.717 (4) Å, which we consider too long to be significant. In this nonacoordination, the central atom is involved in one four-membered nonplanar ring [Rb1/O1^{iii}/C1^{iii}/O2^{iii}; symmetry code: (iii) $-x + \frac{3}{2}, y - \frac{1}{2}, -z + \frac{3}{2}$], in which the largest deviation from the mean plane is 0.1336 (8) Å for atom C1^{iii}. This leads to a notably short distance between the Rb^{I} ion and atom C1 [3.3176 (17) Å]. This steric constraint is probably responsible for the wide range of Rb—O bond lengths [2.8790 (12)–3.3371 (13) Å] and angles [42.82 (3)–158.67 (3)°]. However, the Rb—O distances are close to the expected values for homo- or heterometallic oxalate-based compounds (Dinnebier *et al.*, 2003; Kolitsch, 2004).

On the basis of the first coordination sphere, the resulting coordination polyhedron is a slightly distorted trigonal antiprism exhibiting two planes approximately parallel to each other [the dihedral angle between the sets of atoms O2*W*/O2^{iii}/O1*W* and O4^{ii}/O1^{iii}/O5^{iv} is 7.58 (6)°; all symmetry codes as in Table 1] and an apical cap (O3^{i}). Taking into account the second coordination sphere, the nonacoordination gives an environment which cannot be described in term of a regular dodecahedron, although the dihedral angle between the two trapezoids formed by the sets of atoms O1*W*/O8^{vi}/O1^{iii}/O6^{v} [maximum deviation = 0.0358 (6) Å for atom O1^{iii}] and O4^{ii}/O3^{i}/O2*W*/O2^{iii} [maximum deviation = 0.3724 (6) Å for atom O3^{i}] is 74.53 (2)°, which is near to the ideal value for a dodecahedron having D_2 symmetry (Drew, 1977; Marrot & Trombe, 1993). In this case, atom O5^{iv} constitutes the cap, even

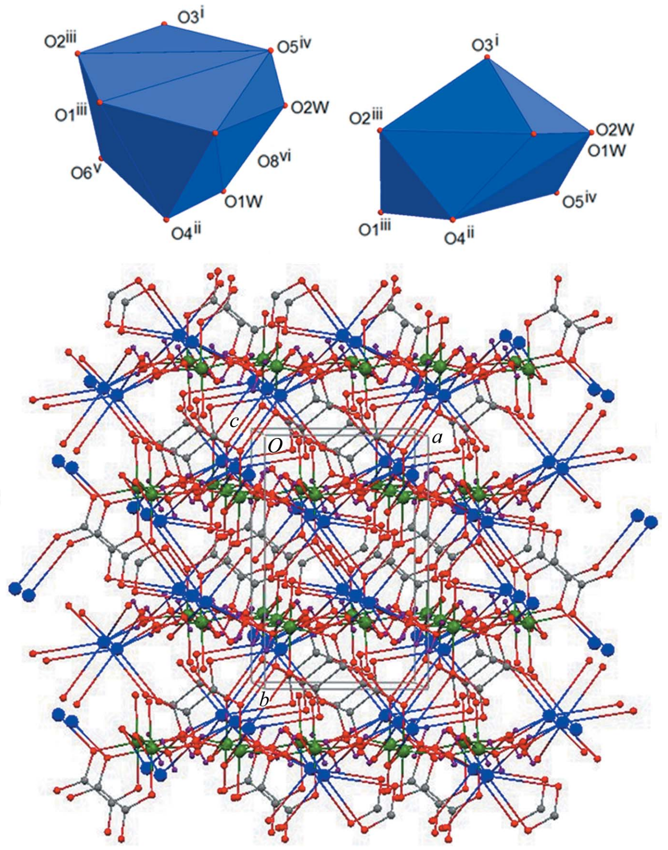

Figure 2
Top: the coordination polyhedra around the Rb atom, taking into account the two coordination spheres (left) or only the first coordination sphere (right). Bottom: a perspective view (ligand *L*2 removed), showing chains running along the *a* and *b* axes. (The symmetry codes are as in Table 1.)

though its distance from the metal atom is not the largest. However, we note that the Rb^I ion is offset and does not lie in the plane of the trapezoids, and that one deviation is too large. As can be seen at the top of Fig. 2, this polyhedron is highly distorted compared with the heptacoordination environment given by the first coordination sphere.

Regarding the $CrO_4(H_2O)_2$ octahedron, it is very slightly distorted, with two longer Cr—O bonds to aqua ligands (Table 1), and with bond angles which are not exactly 90° as a regular octahedral arrangement would imply. This can be explained by the small bite angles of the chelates within each oxalate ligand [82.42 (5) and 82.52 (5)°]. However, the ligand geometries around the metal centre are not distorted. Indeed, unlike $RbO_7(H_2O)_2$, the two chelate rings around Cr^{III} are almost planar; the largest deviations from the mean planes are 0.0221 (9) and 0.0528 (9) Å, respectively, for atoms C4 and O4 of the five-membered rings subtended by ligands *L*1 and *L*2, respectively. Moreover, the smaller ranges of bond lengths [1.9524 (12)–1.9918 (13) Å] and angles [82.42 (5)–96.47 (5)°] are comparable with other oxalates having the same connectivity (Ballester *et al.*, 2001; Kolitsch, 2004; Kahlenberg *et al.*, 2008). In the octahedral environment formed around the Cr^{III} metal centre, the smallest deviation from the mean plane [0.0300 (7) Å for atom O5] is given by a plane which is nearly in the same plane as the η^4-chelate provided by ligand *L*2 and it contains four atoms in equatorial positions (O2*W*/O2/O5/O7), including one water molecule. The other aqua ligand occupies the axial position with atom O4 of one η^4-chelate (*L*1). The Cr^{III} environment indicates significant local symmetry: the chosen equatorial plane and the η^4-chelate provided by *L*2 are nearly in the same plane, the dihedral angle between them being 2.22 (4)°, highlighting the particular arrangement of the two oxalate ligands towards this equatorial plane.

The overall three-dimensional framework, viewed along the *b* axis (Fig. 3), shows the corrugated interpenetrating layers. The Rb^I dodecahedra and the Cr^{III} octahedra share three common vertices belonging to three different oxalate ligands, and one common edge formed by the two aqua ligands. This results in the formation of three different chains of alternating edge- and vertex-shared polyhedra. As depicted at the bottom of Fig. 2 and in Fig. 3, these chains run in a zigzag fashion along the *c* axis *via* an O5 bridge, and along the *b* axis *via* an O2 bridge. Another chain, in which the shortest Rb—Cr distance is observed [4.1192 (3) Å], runs approximately in the *a*-axis direction. Projections of the bipolyhedral chains in the (001) and (100) planes are shown in Fig. 4. In this structure, unlike the homometallic ones studied previously (Kherfi *et al.*, 2010), the oxalate ligands are completely deprotonated, which rules out the building of supramolecular R_d^a synthons (Bernstein *et al.*, 1995). The hydrogen-bonding pattern is due only to water molecules, which act as donors to the O atoms which are not included in the η^4-chelation. The corresponding bonds are strong and nearly linear, forming infinite helical chains (Table 2). However, the unique atom O5, which belongs to one five-membered ring, is involved in a weak hydrogen bond and in a bifurcated hydrogen bond.

A comparison of the title structure with the structurally studied oxalates containing alkali and alkaline earth or transition metals reveals the singular three-dimensional framework of this material. Indeed, the complexes $[KCr(C_2O_4)_2$-

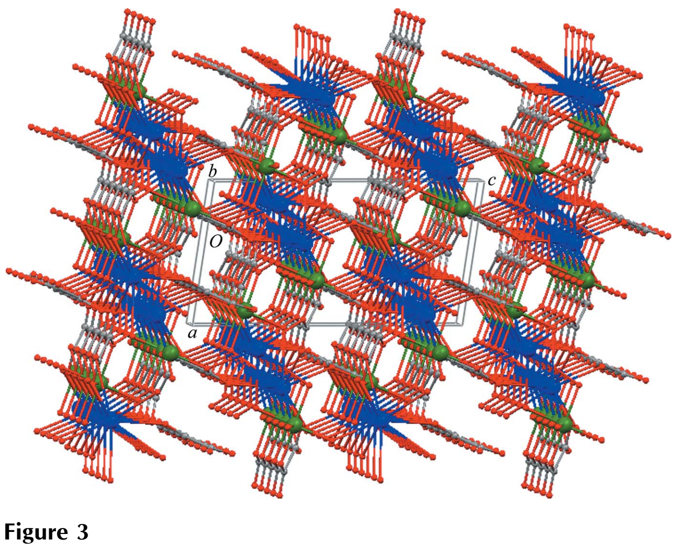

Figure 3
A packing diagram, viewed along [010], showing the corrugated layers.

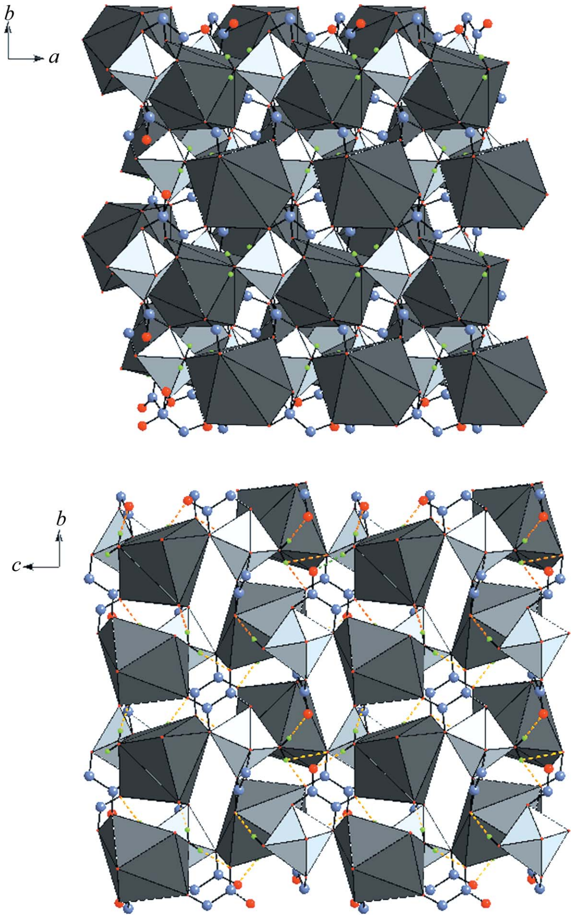

Figure 4
Projections of the bipolyhedra in the (001) and (100) planes. The small polyhedra correspond with the Cr^{III} coordination sphere and the large polyhedra with the full coordination sphere of the Rb^I ion.

$(H_2O)_2]\cdot 3H_2O$ (van Niekerk & Schoening, 1951), $[A_3Cr(C_2O_4)_3]\cdot yH_2O$, with A = K or Rb and y = unknown or 3 (van Niekerk & Schoening, 1952*a*,*b*; Merrachi *et al.*, 1987), $[ACr(C_2O_4)_2]\cdot 2H_2O$, with A = Rb or NH_4 (Kolitsch, 2004; Kahlenberg *et al.*, 2008) and $[A_2M^{II}(C_2O_4)_2]\cdot xH_2O$, with A = K, Rb or Cs and M = Co, Mg or Cu (Viswamitra, 1962; Weichert & Lohn, 1974; Gleizes *et al.*, 1980; Kolitsch, 2004), are all two-dimensional layered structures with the metal ions lying in special positions. Although they belong essentially to monoclinic centrosymmetric space groups ($C2/m$, $P2/c$, $P2_1/c$ and $C2/c$), they display several differing features. In particular, the two isotypic compounds $[RbCr(C_2O_4)_2]\cdot 2H_2O$ (Kolitsch, 2004), studied at room temperature, and $(NH_4)[Cr(C_2O_4)_2]\cdot 2H_2O$ (Kahlenberg *et al.*, 2008), studied at both 173 K and room temperature, elegantly display a close relationship on a microscopic level and show that, from both chemical and structural points of view, the NH_4^+ cation resembles an *s*-block element. However, it presents two disordered orientations, which can be explained by its different role in the structure. It is a counter-ion lying between the layers to accomplish charge balance, while in the title complex the Rb^I ion is included in the building blocks. In the isomeric structure of the title compound studied at room temperature (Kolitsch, 2004), instead of the structure presented here, the water molecules are not bonded to the Rb^I ion but only to the Cr^{III} ion in two apical *trans* positions. Therefore, the two resulting metal coordination polyhedra, RbO_8 and $CrO_4(H_2O)$, have no common edge and the structure consists of alternating layers of Cr^{III} and Rb^I polyhedra connected *via* the unique oxalate ligand. Within the layers, adjacent Cr^{III} octahedra are linked *via* hydrogen bonds and adjacent Rb^I tetragonal prisms form infinite Rb—O—Rb—O chains, as in some typical MOFs. In the present compound, the heterobimetallic Rb—O—Cr—O units are connected into infinite arrays through O-atom bridges and without similar infinite chains. However, the structure can be affiliated to MOFs owing to its secondary building unit and its empty voids (Tranchemontagne *et al.*, 2009).

From a structural point of view, the compound presented here, studied at 100 K, can be considered as a supramolecular isomer (Robin & Fromm, 2006) of the compound having the same chemical formula and found to crystallize at room temperature in the space group $C2/m$ (Kolitsch, 2004). The novel structural arrangement observed here, highlighting interpenetrated layers, might be the consequence of the hydrothermal synthesis conditions, which result in a higher dimensionality and density.

Experimental

A mixture of rubidium carbonate (0.173 g, 0.75 mmol), chromium nitrate nonahydrate (0.200 g, 0.5 mmol) and oxalic acid dihydrate (0.189 g, 1.5 mmol) in deionized water (15 ml) was introduced into a 23 ml Teflon-lined stainless steel vessel. The vessel was sealed and heated at 393 K for one week. Dark-pink single crystals of suitable size were obtained after cooling the vessel to room temperature; they were filtered off and washed with diethyl ether.

Table 1
Selected geometric parameters (Å, °).

$Rb1—O3^{i}$	2.8790 (12)	Cr1—O2*W*	1.9814 (13)
$Rb1—O4^{ii}$	2.9287 (12)	Cr1—O1*W*	1.9918 (13)
$Rb1—O2^{iii}$	2.9711 (12)	C1—O1	1.222 (2)
$Rb1—O5^{iv}$	2.9849 (12)	C1—O2	1.289 (2)
Rb1—O2*W*	3.0778 (13)	C2—O3	1.232 (2)
Rb1—O1*W*	3.1053 (13)	C2—O4	1.289 (2)
$Rb1—O1^{iii}$	3.1054 (13)	C3—O6	1.228 (2)
$Rb1—O6^{v}$	3.2089 (12)	C3—O5	1.291 (2)
$Rb1—O8^{vi}$	3.3371 (13)	C4—O8	1.223 (2)
Cr1—O2	1.9524 (12)	C4—O7	1.287 (2)
Cr1—O4	1.9600 (12)	C1—C2	1.547 (2)
Cr1—O7	1.9615 (12)	C3—C4	1.549 (2)
Cr1—O5	1.9665 (12)		
O1—C1—O2	124.42 (16)	O6—C3—O5	125.14 (15)
O1—C1—C2	122.48 (16)	O6—C3—C4	121.41 (15)
O2—C1—C2	113.11 (14)	O5—C3—C4	113.45 (14)
O3—C2—O4	124.81 (16)	O8—C4—O7	125.34 (16)
O3—C2—C1	121.22 (15)	O8—C4—C3	121.27 (15)
O4—C2—C1	113.96 (14)	O7—C4—C3	113.38 (14)
O1—C1—C2—O3	5.4 (3)	O6—C3—C4—O8	15.9 (2)
O2—C1—C2—O3	−175.04 (15)	O5—C3—C4—O8	−164.59 (16)
O1—C1—C2—O4	−175.92 (16)	O6—C3—C4—O7	−165.22 (15)
O2—C1—C2—O4	3.6 (2)	O5—C3—C4—O7	14.3 (2)

Symmetry codes: (i) $-x+\frac{1}{2}, y-\frac{1}{2}, -z+\frac{3}{2}$; (ii) $x+1, y, z$; (iii) $-x+\frac{3}{2}, y-\frac{1}{2}, -z+\frac{3}{2}$; (iv) $x+\frac{1}{2}, -y+\frac{1}{2}, z+\frac{1}{2}$; (v) $-x+1, -y, -z+1$; (vi) $-x+\frac{3}{2}, y+\frac{1}{2}, -z+\frac{3}{2}$.

Crystal data

$[CrRb(C_2O_4)_2(H_2O)_2]$
M_r = 349.54
Monoclinic, $P2_1/n$
a = 6.8506 (1) Å
b = 10.521 (1) Å
c = 12.6995 (2) Å
β = 98.773 (2)°
V = 904.61 (9) Å^3
Z = 4
Mo $K\alpha$ radiation
μ = 6.66 mm^{-1}
T = 100 K
0.3 × 0.2 × 0.2 mm

Data collection

Oxford Xcalibur diffractometer
Absorption correction: numerical [*CrysAlis RED* (Oxford Diffraction, 2009), based on expressions derived by Clark & Reid (1995)]
T_{min} = 0.221, T_{max} = 0.264
18885 measured reflections
2178 independent reflections
1938 reflections with $I > 2\sigma(I)$
R_{int} = 0.033
3 standard reflections every 100 reflections
intensity decay: 0.01%

Refinement

$R[F^2 > 2\sigma(F^2)]$ = 0.016
$wR(F^2)$ = 0.044
S = 1.06
2178 reflections
161 parameters
6 restraints
All H-atom parameters refined
$\Delta\rho_{max}$ = 0.44 e Å^{-3}
$\Delta\rho_{min}$ = −0.46 e Å^{-3}

Table 2
Hydrogen-bond geometry (Å, °).

D—H···*A*	*D*—H	H···*A*	*D*···*A*	*D*—H···*A*
O1*W*—H1···$O8^{v}$	0.79 (2)	1.86 (2)	2.6301 (18)	167
O1*W*—H2···$O3^{ii}$	0.79 (2)	1.91 (2)	2.6832 (18)	167
O2*W*—H3···$O6^{iv}$	0.80 (2)	1.88 (2)	2.6641 (17)	169
O2*W*—H3···$O5^{iv}$	0.80 (2)	2.58 (2)	2.9641 (17)	111
O2*W*—H4···$O1^{i}$	0.78 (2)	1.87 (2)	2.6410 (18)	171

Symmetry codes: (i) $-x+\frac{1}{2}, y-\frac{1}{2}, -z+\frac{3}{2}$; (ii) $x+1, y, z$; (iv) $x+\frac{1}{2}, -y+\frac{1}{2}, z+\frac{1}{2}$; (v) $-x+1, -y, -z+1$.

Water H atoms were located in a difference Fourier map and refined with a restrained O—H distance of 0.85 (5) Å. The highest electron density in the final difference Fourier map is 0.77 Å from atom C1 and the deepest hole is 0.39 Å from the Cr^{III} ion.

Data collection: *CrysAlis CCD* (Oxford Diffraction, 2009); cell refinement: *CrysAlis RED* (Oxford Diffraction, 2009); data reduction: *CrysAlis RED*; program(s) used to solve structure: *SHELXS97* (Sheldrick, 2008); program(s) used to refine structure: *SHELXL97* (Sheldrick, 2008); molecular graphics: *ORTEP-3 for Windows* (Farrugia, 1997); software used to prepare material for publication: *WinGX* (Farrugia, 1999).

The authors thank E. Wenger, Service Commun de Diffractométrie, Nancy University, for the X-ray data collection. We are grateful for financial support from the CMEP project of the TASSILI programme (O5 MDU-France, MESRS, Algeria).

Supplementary data and figures for this paper are available from the IUCr electronic archives (Reference: JZ3199). Services for accessing these data are described at the back of the journal.

References

Aliouane, K., Rahahlia, N., Guehria-Laidoudi, A., Dahaoui, S. & Lecomte, C. (2007). *Acta Cryst.* E**63**, m1834–m1836.

Audebrand, N., Raite, S. & Louër, D. (2003). *Solid State Sci.* **5**, 783–794.

Ballester, G., Coronado, C., Giménez-Saiz, C. & Romero, F. M. (2001). *Angew. Chem. Int. Ed.* **40**, 792–795.

Bernstein, J., Davis, R. E., Shimoni, L. & Chang, N.-L. (1995). *Angew. Chem. Int. Ed. Engl.* **34**, 1555–1573.

Cheetham, A. K., Rao, C. N. R. & Keller, R. K. (2006). *Chem. Commun.* pp. 4780–4795.

Clark, R. C. & Reid, J. S. (1995). *Acta Cryst.* A**51**, 887–897.

Coronado, E., Delhaes, P., Gatteschi, D. & Miller, J. S. (1996). *Molecular Magnetism: From Molecular Assemblies to the Devices*. Dordrecht: Kluwer Academic Publishers.

Czaja, A. U., Trukhan, N. & Müller, U. (2009). *Chem. Soc. Rev.* **38**, 1284–1293.

Dinnebier, R. E., Vensky, S., Panthöfer, M. & Jansen, M. (2003). *Inorg. Chem.* **42**, 1499–1507.

Djehni, S., Balegroune, F., Guehria-Laidoudi, A., Dahaoui, S. & Lecomte, C. (2007). *Acta Cryst.* C**63**, m91–m93.

Drew, M. G. B. (1977). *Coord. Chem. Rev.* **24**, 179–275.

Farrugia, L. J. (1997). *J. Appl. Cryst.* **30**, 565.

Farrugia, L. J. (1999). *J. Appl. Cryst.* **32**, 837–838.

Gleizes, A., Maury, F. & Galy, J. (1980). *Inorg. Chem.* **19**, 2074–2078.

Hoskins, B. F. & Robson, R. (1990). *J. Am. Chem. Soc.* **112**, 1546–1554.

Janiak, C. (2003). *Dalton Trans.* pp. 2781–2804.

Kahlenberg, V., Wertl, W., Kremenovic, A., Schuster, P. & Schottenberger, H. (2008). *Z. Anorg. Allg. Chem.* **634**, 921–926.

Kherfi, H., Hamadene, M., Guehria-Laïdoudi, A., Dahaoui, S. & Lecomte, C. (2010). *Materials*, **3**, 1281–1301.

Kolitsch, U. (2004). *Acta Cryst.* C**60**, m129–m133.

Marrot, F. & Trombe, J. C. (1993). *C. R. Acad. Sci. Ser. II*, **317**, 319–324.

Merrachi, E. H., Mentzen, B. F. & Chassagneux, F. (1987). *Rev. Chim. Miner.* **24**, 427–445.

Mosaad, M. M., El-Shawarby, A., El-Tanahy, Z. H. & Abdel-Kader, M. M. (1995). *J. Mater. Sci. Mater. Electron.* **6**, 235–239.

Murray, L. J., Dinca, M. & Long, J. R. (2009). *Chem. Soc. Rev.* **38**, 1294–1314.

Niekerk, J. N. van & Schoening, F. R. L. (1951). *Acta Cryst.* **4**, 35–41.

Niekerk, J. N. van & Schoening, F. R. L. (1952*a*). *Acta Cryst.* **5**, 196–202.

Niekerk, J. N. van & Schoening, F. R. L. (1952*b*). *Acta Cryst.* **5**, 475–476.

Oxford Diffraction (2009). *CrysAlis CCD* and *CrysAlis RED*. Oxford Diffraction Ltd, Yarnton, Oxfordshire, England.

Price, D. T., Powell, A. K. & Wood, P. T. (2003). *Dalton Trans.* pp. 2478–2482.

Rahahlia, N., Benmerad, B., Guehria-Laïdoudi, A., Dahaoui, S. & Lecomte, C. (2007). *J. Mol. Struct.* **833**, 42–48.

Rao, C. N. R., Natarajan, S. & Vaidhyanathan, R. (2004). *Angew. Chem. Int. Ed.* **43**, 1466–1496.

Robin, A. Y. & Fromm, K. M. (2006). *Coord. Chem. Rev.* **250**, 2127–2157.

Robinson, F. & Zaworotko, M. J. (1995). *J. Chem. Soc. Chem. Commun.* pp. 2413–2414.

Schaack, G. (1990). *Ferroelectrics*, **104**, 147–158.

Sheldrick, G. M. (2008). *Acta Cryst.* A**64**, 112–122.

Tranchemontagne, D. J., Mendoza-Cortés, J. L., O'Keefe, M. & Yaghi, O. M. (2009). *Chem. Soc. Rev.* **38**, 1257–1283.

Uemura, T., Yanai, N. & Kitagawa, S. (2009). *Chem. Soc. Rev.* **38**, 1228–1236.

Viswamitra, M. A. (1962). *J. Chem. Phys.* **37**, 1408–1414.

Wang, Z. & Cohen, S. M. (2009). *Chem. Soc. Rev.* **38**, 1315–1329.

Weichert, T. & Lohn, J. (1974). *Z. Kristallogr.* **139**, 223–235.

Yaghi, O. M. & Li, H. (1996). *J. Am. Chem. Soc.* **118**, 295–296.

Zhang, X. M., Zhang, X. H., Wu, H. S., Tong, M. L. & Neg, S. W. (2008). *Inorg. Chem.* **47**, 7462–7464.